Sanguinarine Blocks Cytokinesis in Bacteria by Inhibiting FtsZ Assembly and Bundling†

Tushar K. Beuria, Manas K. Santra, and Dulal Panda*

School of Biosciences and Bioengineering, Indian Institute of Technology Bombay, Mumbai 400076, India

Received April 27, 2005; Revised Manuscript Received August 29, 2005

ABSTRACT: Bacterial diseases are among the leading causes of human death. The development of antibiotic resistance greatly contributes to the high mortality rate, and thus, the discovery of antibacterial drugs with novel mechanisms of action is needed. In this study, we found that sanguinarine, a benzophenanthridine alkaloid, strongly induced filamentation in both Gram-positive and Gram-negative bacteria and prevented bacterial cell division by inhibiting cytokinesis. Sanguinarine did not perturb the membrane structure in *Escherichia coli*. However, it perturbed the cytokinetic Z-ring formation in *E. coli*. In addition, sanguinarine strongly reduced the frequency of the occurrence of Z rings/micrometer of *Bacillus subtilis* length but did not alter the number of nucleoids/micrometer of cell length. The results suggested that sanguinarine inhibited cytokinesis in *B. subtilis* by inhibiting Z-ring formation without affecting nucleoid segregation. Sanguinarine inhibited the assembly of purified FtsZ and reduced the bundling of FtsZ protofilaments *in vitro*. Further, the interaction of sanguinarine to FtsZ was investigated using size-exclusion chromatography, an extrinsic fluorescent probe 1-anilinonaphthalene-8-sulfonic acid, and tryptophan fluorescence of mutated FtsZ (Y371W). Sanguinarine was found to bind to FtsZ with a dissociation constant of 18−30 μM. The results together show that sanguinarine inhibits bacterial division by perturbing FtsZ assembly dynamics in the Z ring and provide evidence in support of the hypothesis that the assembly and bundling of FtsZ play a critical role in bacterial cytokinesis. The results suggest that sanguinarine may be used as a lead compound to develop FtsZ-targeted antibacterial agents.

FtsZ is a key protein involved in prokaryotic cell division (*1*, *2*). Bacterial cell division occurs at the site of formation of the cytokinetic Z ring, which is a dynamic polymeric structure composed of FtsZ subunits (*3*). The indispensability of FtsZ has been established from a number of genetic studies (*4*−*7*). While a null mutation in the *ftsZ* gene was found to be lethal, its discovery was attributed to a temperature-sensitive allele (*ftsZ84*) found to cause disassembly of the cytokinetic Z rings and the formation of filamentous cells that are incapable of dividing at nonpermissive temperature (*8*). FtsZ in the Z ring undergoes a rapid and continuous turnover with its soluble pool, and it is thought that the assembly dynamics of the Z ring may play a role in the functioning of the septum (*3*, *9*). Therefore, inhibitors of the Z ring are thought to have clinical potential against pathogenic bacteria. Recently, a few small molecule inhibitors of FtsZ assembly have been reported to possess antibacterial activity, but their effects on the Z-ring assembly *in vivo* were not tested (*10*−*12*). Most recently, zantrins, a group of small molecules of diverse structure, which either inhibited or stabilized FtsZ assembly *in vitro*, were shown to perturb Z-ring assembly in bacteria (*13*). Although it is reasonable to think that the inhibitors of the Z ring that block cytokinesis in bacteria would induce filamentation, none of the zantrins except Z5 induced filament formation in *Escherichia coli* (*13*). Therefore, the relationship between Z-ring perturbation and filamentation is not clear.

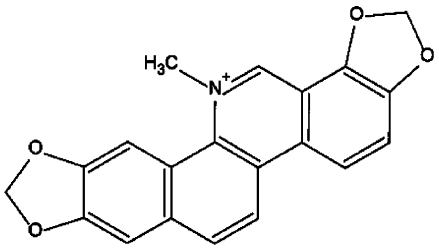

FIGURE 1: Structure of sanguinarine [13-methyl-(1,3)-benzodioxolo-(5,6-*c*)1,3-dioxolo-(4,5-*i*)phenanthridinium].

The assembly and bundling of FtsZ protofilaments are considered to be essential for the construction and functioning of the cytokinetic Z ring during bacterial division (*14*−*16*); therefore, the assembly and bundling of FtsZ protofilaments may be used as a screen to find FtsZ-targeted antibacterial agents. In addition, an inhibitor of the assembly and bundling of FtsZ protofilaments can be used as a tool to understand the linkage between perturbation of FtsZ assembly dynamics, inhibition of Z-ring formation and function, and inhibition of bacterial proliferation.

Sanguinarine (Figure 1), a benzophenanthridine alkaloid derived from the rhizomes of *Sanguinaria canadensis*, has a wide range of antimicrobial activity (*17*). It is used in a broad range of oral health products including toothpaste to

† This work is supported by a grant from the Department of Science and Technology, Government of India (to D.P.).

* To whom correspondence should be addressed: School of Biosciences and Bioengineering, Indian Institute of Technology Bombay, Mumbai 400076, India. Telephone: 91-22-2576-7838. Fax: 91-22-2572-3480. E-mail: panda@iitb.ac.in.

10.1021/bi050767+ CCC: $30.25
Published on Web 11/22/2005

prevent dental plaque formation. In addition, sanguinarine is also known to inhibit proliferation of various types of cancer cells (*18*, *19*), and sanguinarine has been shown to be preferentially active against cancer cells as compared to the normal cells (*19*). Interestingly, sanguinarine also inhibits tubulin assembly into microtubules *in vitro* and in mammalian cells (*20*, *21*; M. Lopus and D. Panda, unpublished data). Because FtsZ is a prokaryotic homologue of tubulin (*22*−*27*), we wanted to investigate whether sanguinarine inhibits cytokinesis in bacteria by perturbing FtsZ assembly.

We found that sanguinarine inhibited proliferation of both Gram-positive and Gram-negative bacteria by blocking cytokinesis without affecting DNA replication or nucleoid segregation. Our data provide evidence that sanguinarine inhibits bacterial cytokinesis by perturbing the assembly and function of the Z ring in bacteria by inhibiting FtsZ assembly through FtsZ binding. Finally, our results support the idea that FtsZ may be an excellent target of antibacterial drugs with a new mechanism of action.

EXPERIMENTAL PROCEDURES

Materials. Piperazine-*N*,*N*′-bis(2-ethane sulfonic acid) (pipes),[1] monosodium glutamate, isopropyl-β-D-thiogalactopyranoside (IPTG), bovine serum albumin (BSA), GTP, 6-diamidino-2-phenylindole (DAPI), and Cy3-conjugated goat anti-rabbit secondary antibody were obtained from Sigma Chemical Company. 1-Anilinonaphthalene-8-sulfonic acid (ANS) and FM 4−64 were purchased from Molecular Probes, Eugene, OR. Primary polyclonal anti-FtsZ rabbit antibody was developed in rabbit against *E. coli* FtsZ by Bangalore Genie, India. All other chemicals used were of analytical grade.

FtsZ Expression and Purification. Recombinant *E. coli* FtsZ was overexpressed and purified from *E. coli* BL21 strain as described previously (*28*−*30*). The FtsZ concentration was measured by the Bradford method using BSA as a standard (*31*). The purified protein was frozen and stored at −80 °C. Prior to use, FtsZ was thawed and centrifuged at 287000*g* for 30 min to remove insoluble aggregates.

FtsZ does not have a tryptophan residue but has three tyrosine residues. We replaced tyrosine-371, which is located at the extreme C terminus of FtsZ, by a tryptophan residue. Site-directed mutagenesis on FtsZ was performed using Stratagene Quick-Change mutagenesis kit (catalog number 200518) with the FtsZ expression plasmid pET11a as a template (*32*). The mutation (Y371W) was confirmed by DNA sequencing (Microsynth, Switzerland). The mutant protein FtsZ (Y371W) was expressed in *E. coli* BL21 (DE3) and purified as described for the native protein.

Light-Scattering Assay. A light-scattering assay was performed as described previously (*28*). Briefly, FtsZ (6 μM) in 25 mM pipes buffer (pH 6.8) was incubated with different concentrations (25−100 μM) of sanguinarine for 10 min on ice. The reaction mixtures were polymerized in the presence of 1 M glutamate, 10 mM $MgSO_4$, and 1 mM GTP at 37 °C. GTP was added as the last fraction. The rate and extent of polymerization were measured by 90° light scattering at 600 nm using a JASCO 6500 spectrofluorimeter.

Sedimentation Assay. FtsZ (12 μM) in 25 mM pipes buffer (pH 6.8) was incubated with different concentrations (25−50 μM) of sanguinarine for 10 min on ice. Then, 10 mM $MgSO_4$ and 1 mM GTP were added to the reaction mixtures and incubated for an additional 15 min at 37 °C. Polymeric FtsZ was sedimented at 287000*g* for 30 min, and the protein concentration in the supernatant was measured. The protein concentration in the pellet was calculated by subtracting the concentration of protein in the supernatant from the total protein (*28*).

Electron Microscopy. FtsZ was polymerized in the absence and presence of different concentrations of sanguinarine as described in the light-scattering experiment. After 10 min of assembly, FtsZ polymers were fixed with 0.5% glutaraldehyde and transferred onto formvar-carbon-coated copper grids (300 mesh size). The samples were negatively stained with 1% uranyl acetate and observed by electron microscopy (FEI TECHNAI G^2 12) (*28*).

Binding of Sanguinarine to FtsZ. FtsZ (1 μM) was first incubated with different concentrations of sanguinarine. Then, 30 μM ANS was added to the reaction mixture and incubated for an additional 10 min at 25 °C. Sanguinarine was found to decrease FtsZ−ANS complex fluorescence in a concentration-dependent manner. The binding constant of sanguinarine to FtsZ was calculated from the decrease in fluorescence intensity using a double-reciprocal curve analysis (*33*). To reduce inner-filter effects at high concentrations of sanguinarine, a 3 mm path-length cell was used to measure fluorescence. The inner-filter effect was minimal, and it was corrected as described previously (*33*). The fraction of the binding sites (X) occupied by sanguinarine was determined using the equation $X = (F_o - F)/\Delta F_{max}$, where F_o is the fluorescence intensity of FtsZ−ANS in the absence of sanguinarine, F is the corrected fluorescence intensity of FtsZ−ANS in the presence of sanguinarine, and ΔF_{max} was calculated from the plot of $1/(F_o - F)$ versus 1/[sanguinarine] and extrapolating 1/[sanguinarine] to 0. The dissociation constant (K_d) was determined using the relationship, $1/X = 1 + K_d/L_f$, where L_f represents the free sanguinarine concentration, and $L_f = C - X[Y]$, where C is total concentration of sanguinarine and $[Y]$ is the molar concentration of ligand-binding sites assuming a single binding site/FtsZ monomer. The excitation and emission wavelengths were 370 and 470 nm, respectively. Sanguinarine displayed negligible fluorescence upon excitation at 370 nm, and the corrected data were used for all calculation.

Binding of ANS to FtsZ. The dissociation constant of ANS binding to FtsZ was determined by incubating FtsZ (1 μM) with different concentrations (2−50 μM) of ANS in 25 mM sodium phosphate buffer at pH 6.8 and 25 °C for 30 min as described previously (*30*). The dissociation constant of ANS binding to FtsZ was also determined in the presence of 25 and 60 μM sanguinarine. FtsZ was incubated with either 25 or 60 μM sanguinarine for 30 min and further incubated with different concentrations of ANS for an additional 30 min. The excitation and emission wavelengths were 370 and 480 nm, respectively. A cell of 0.3 cm path length was used to determine fluorescence intensity changes.

[1] Abbreviations: pipes, piperazine-*N*,*N*′-bis(2-ethane sulfonic acid); IPTG, isopropyl-β-D-thiogalactopyranoside; BSA, bovine serum albumin; DAPI, 6-diamidino-2-phenylindole; ANS, 1-anilinonaphthalene-8-sulfonic acid.

FtsZ (Y371W) (1 μM) was incubated with different concentrations (5−60 μM) of sanguinarine at 25 °C for 30 min. When excited at 290 nm, FtsZ (Y371W) displayed a typical emission spectrum with a maximum at 340 nm and sanguinarine reduced intrinsic fluorescence of FtsZ (Y371W). The apparent decrease in the fluorescence values in the presence of varying concentrations of sanguinarine were corrected for the inner-filter effect as described previously (*33*). The corrected fluorescence intensities of FtsZ (Y371W) in the presence of different concentrations of sanguinarine were used to determine the dissociation constant as stated in the previous paragraph (*33*, *34*).

Determination of Antibacterial Activity of Sanguinarine. Bacteria were grown in the absence and presence of different concentrations of sanguinarine in Luria−Bertani (LB) media (10 g/L tryptone, 5 g/L yeast extract, and 10 g/L NaCl) for 3 h. The inhibitory effect of sanguinarine on the bacterial division was determined by measuring the absorbance at 600 nm (A_{600}). The half-maximal inhibitory concentration (IC_{50}) was calculated by plotting A_{600} against the sanguinarine concentration. In the case of *B. subtilis* 168, IC_{50} was also calculated by counting the bacterial cells at different concentrations of sanguinarine by light microscopy and was found to be similar to the IC_{50} value obtained by the absorbance method.

Visualization of Bacterial Morphology. B. subtilis 168 or *E. coli* BL21 were inoculated in LB media containing different concentrations of sanguinarine and grown overnight. *B. subtilis* 168 cells were fixed with 0.04% glutaraldehyde plus 2.5% formaldehyde, harvested, and resuspended in LB medium containing 0.25% of agarose. A total of 5 μL of the suspension was placed on a cover slip, and morphology of the bacterial cells was observed under light microscope. FM 4−64 was added to 1 mL of growing *E. coli* BL21 culture to a final concentration of 1−1.5 μM. After 15 min, cells were observed using a microscope (Nikon ECLIPSE TE2000-U) with a 60× objective. The images were captured using a CoolSNAP-Pro camera, and the length of a bacterial cell was measured by using IMAGEPRO PLUS software (Media Cybernetics, Silver Spring, MD).

Visualization of Z Ring in the Bacteria. An overnight culture of *E. coli* JM109 WM647 (a gift from Dr. W. Margolin) containing an IPTG-inducible plasmid for the production of GFP-tagged FtsZ was diluted to 1% in the LB media containing different concentrations of sanguinarine and 40 μM IPTG (*35*). Cells were grown for 4 h, fixed, harvested, and resuspended in LB medium containing 0.25% of agarose, and visualized by a fluorescence microscope (60× objective).

Immunofluorescence Microscopy. B. subtilis 168 was immunostained with the procedure described earlier (*36*). Briefly, *B. subtilis* 168 ($A_{600} \sim 0.3-0.4$) cells were treated with different concentrations of sanguinarine for 90 min and then fixed with 2.5% formaldehyde and 0.04% glutaraldehyde. Cellular FtsZ was stained with a polyclonal anti-FtsZ rabbit antibody (Bangalore Genie, India) followed by a Cy3-conjugated goat anti-rabbit secondary antibody (Sigma) and visualized under a fluorescence microscope (Nikon ECLIPSE TE2000-U). Nucleoids were visualized by treating the cells with 0.5 μg/mL DAPI. Sanguinarine did not display background fluorescence.

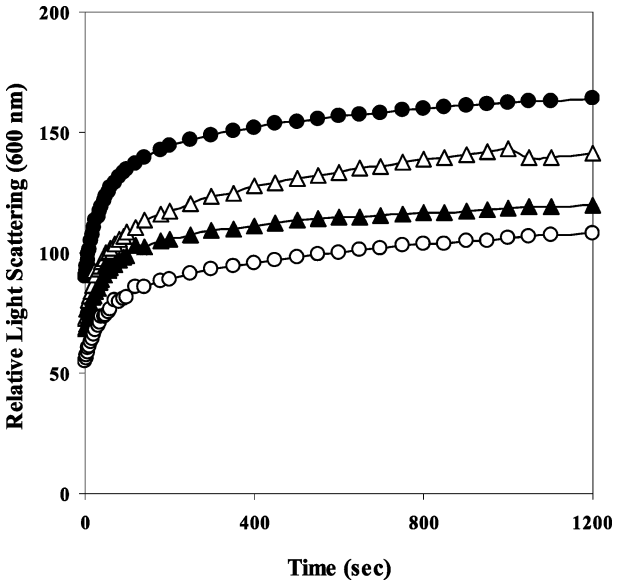

FIGURE 2: Sanguinarine inhibited the rate and extent of FtsZ assembly. FtsZ (6 μM) was polymerized with 1 M glutamate, 10 mM $MgSO_4$, and 1 mM GTP at 37 °C in the absence and presence of different concentrations (25−100 μM) of sanguinarine, and the rate and extent of the assembly reaction were monitored at 600 nm. Shown are assembly reactions in the absence of sanguinarine (●) and in the presence of 25 μM (△), 50 μM (▲), and 100 μM (○) sanguinarine.

RESULTS

Inhibition of FtsZ Assembly and Protofilament Bundling by Sanguinarine. The effects of sanguinarine on the kinetics of FtsZ assembly *in vitro* are shown in Figure 2. The light-scattering traces show that the assembly of FtsZ occurs in two steps (Figure 2), which is consistent with the suggestion that FtsZ monomers first polymerize into protofilaments, and subsequently, bundling of protofilaments produces multi-stranded FtsZ polymers (*28*, *29*). Sanguinarine strongly inhibited the development of the light-scattering signal of FtsZ assembly, suggesting that it inhibited FtsZ assembly and/or the bundling of assembled FtsZ protofilaments. In the absence of sanguinarine, a dense network of thick bundles of FtsZ polymers was observed by electron microscopy (Figure 3). Sanguinarine inhibited FtsZ bundle formation (Figure 3). For example, the average thickness of the FtsZ bundles was 72 ± 29, 59 ± 18, and 51 ± 16 nm in the absence and presence of 50 and 100 μM sanguinarine, respectively. The observed differences in bundle thickness in the absence and presence of 50 and 100 μM sanguinarine were found to be significant at a 99.9% confidence level ($p < 0.001$). Further, sanguinarine-treated FtsZ polymers were also significantly shorter in length as compared to control polymers (Figure 3). In the presence of 100 μM sanguinarine, FtsZ formed short bundles with mean lengths of 2.3 ± 1.2 μm compared to the FtsZ protofilaments formed in the absence of sanguinarine, which were bigger than the field of view (5.4 × 6.7 μm). Again, at high concentrations, sanguinarine induced aggregation of FtsZ monomers.

The effects of sanguinarine on the polymer mass of FtsZ were also determined by sedimentation. FtsZ (12 μM) was polymerized in the presence of 10 mM $MgSO_4$ and 1 mM GTP with or without sanguinarine. Sanguinarine reduced the polymer mass of FtsZ in a concentration-dependent manner. For example, 72 ± 3, 62 ± 5, and 54 ± 6% of the total

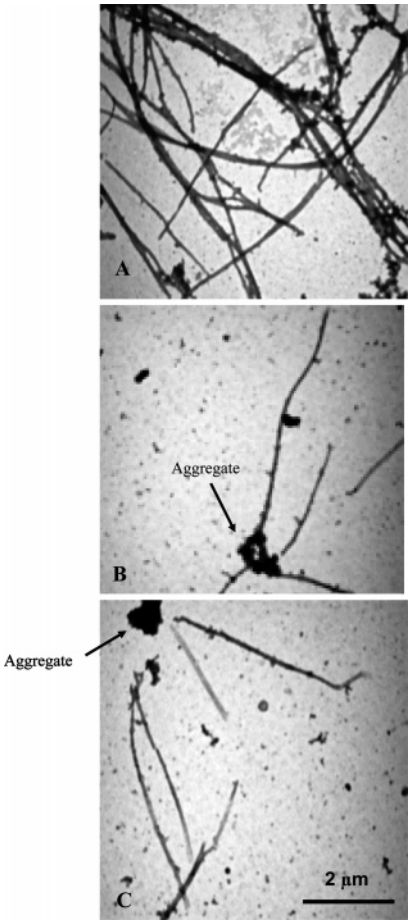

FIGURE 3: Electron micrographs of FtsZ polymers. FtsZ (6 μM) was polymerized with 1 M glutamate, 10 mM $MgSO_4$, and 1 mM GTP at 37 °C in the absence and presence of different concentrations (50 and 100 μM) of sanguinarine. A, B, and C show electron micrographs of FtsZ polymers in the absence and presence of 50 and 100 μM sanguinarine, respectively. A *t*-test analysis showed that the differences in bundle thickness in the absence and presence of 50 and 100 μM sanguinarine are significant at a level of 99.9% ($p < 0.001$). Arrows in the case of B and C show aggregates of FtsZ. The scale bar is 2 μm.

FtsZ were pelleted as polymers in the absence and presence of 25 and 50 μM sanguinarine, respectively. Under these conditions, sanguinarine also inhibited the bundling of FtsZ protofilaments. For example, the thickness of the protofilaments were found to be 41 ± 14 and 25 ± 9 nm ($p < 0.001$) in the absence and presence of 50 μM sanguinarine, respectively (data not shown).

Sanguinarine Binds to FtsZ. Using size-exclusion chromatography, sanguinarine was found to coelute with FtsZ, suggesting that it binds to FtsZ (Figure 4A). The fluorescence intensity of sanguinarine did not change upon binding to FtsZ; therefore, sanguinarine fluorescence could not be used to determine the binding constant for the binding of sanguinarine to FtsZ. Hydrophobic probes are routinely used to determine ligand interactions with proteins (*33*). ANS was shown to bind to FtsZ (*30*, *37*), and the binding of ANS to FtsZ did not inhibit FtsZ assembly (*37*). Thus, we used the hydrophobic fluorescent probe ANS to calculate the dissociation constant (K_d) of the interaction of FtsZ with sanguinarine. Sanguinarine reduced FtsZ−ANS fluorescence in a concentration-dependent manner (Figure 4B). The K_d for the binding of sanguinarine to FtsZ was determined to be 30 ± 6 μM using a double-reciprocal plot of the fluorescence data (inset of Figure 4B).

Intrinsic tryptophan fluorescence of proteins has also been widely used to determine ligand binding to proteins (*34*). However, FtsZ does not have any tryptophan residues. We constructed a mutated FtsZ (Y371W) by replacing the tyrosine residue at position 371 with a tryptophan residue. The assembly kinetics of the native and mutant FtsZ was found to be similar by 90° light scattering (Figure 4C). Under similar conditions, the sedimentable polymer mass was determined to be 68 ± 1.5 and 69 ± 2% for the native and mutated proteins, respectively. The results show that the mutation did not alter the polymerization ability of FtsZ. We used the intrinsic tryptophan fluorescence of the mutated FtsZ (Y371W) to determine the binding constant of sanguinarine and FtsZ interaction. Sanguinarine quenched tryptophan fluorescence of FtsZ (Y371W) in a concentration-dependent manner (Figure 4D), and a dissociation constant of 18.4 ± 1.6 μM for the interaction was determined using a double-reciprocal plot (inset of Figure 4D).

Sanguinarine quenched FtsZ−ANS fluorescence in a concentration-dependent manner (Figure 4B); therefore, we examined whether sanguinarine might bind to FtsZ at the ANS-binding site. The K_d of ANS binding to FtsZ was determined to be 37.4 ± 6.0, 37.1 ± 4.5, and 34.7 ± 7.3 μM in the absence and presence of 25 and 60 μM sanguinarine, respectively. The results suggested that sanguinarine did not bind to FtsZ at the ANS site.

Sanguinarine Inhibited Cell Proliferation and Induced Filamentation in Bacteria. Sanguinarine inhibited proliferation of *B. subtilis* 168, *E. coli* BL21, and *E. coli* JM109 (WM647) with widely different potencies. For example, the half-maximal inhibitory concentrations (IC_{50}) were found to be 3 ± 1, 14 ± 2.3, and 36 ± 5.1 μM for *B. subtilis* 168, *E. coli* BL21 (wild), and *E. coli* JM109 (WM647), respectively. The growth of *B. subtilis* was completely inhibited in the presence of 10 μM sanguinarine, while 75 μM sanguinarine completely inhibited *E. coli* (Bl21) wild strain growth. Sanguinarine was found to induce filamentation in the bacteria (Figure 5). For example, overnight treatment of sanguinarine (5 μM) decreased the proliferation of *B. subtilis* 168 by 82% and increased the length of the bacteria by 5-fold from 2.6 ± 0.2 to 14.2 ± 0.9 μm. Similarly, overnight treatment of sanguinarine (18 μM) also increased the length of *E. coli* BL21 by 8-fold, indicating that sanguinarine also inhibited cytokinesis of *E. coli*. Because perturbation of the membrane structure can induce cell lysis, we examined the effects of sanguinarine on the membrane structure. The effect of sanguinarine on the membrane structure of FtsZ was determined by comparing the fluorescence intensities of FM 4−64 across the membrane of *E. coli* Bl21 strain in the absence and presence of sanguinarine (parts C and D of Figure 5). The fluorescence intensities across the membrane of *E. coli* were found to be 1885 ± 300 and 1835 ± 440 arbitrary units in the absence and presence of 18 μM sanguinarine, respectively. The result suggested that sanguinarine did not affect the membrane structure in *E. coli*.

In rod-shaped bacteria, septum formation during cell division is engineered by the dynamic Z ring, and recent evidence indicates that perturbation of the Z ring inhibits cell division and increases the bacterial length (*4*, *38*). Sanguinarine was found to inhibit FtsZ assembly and

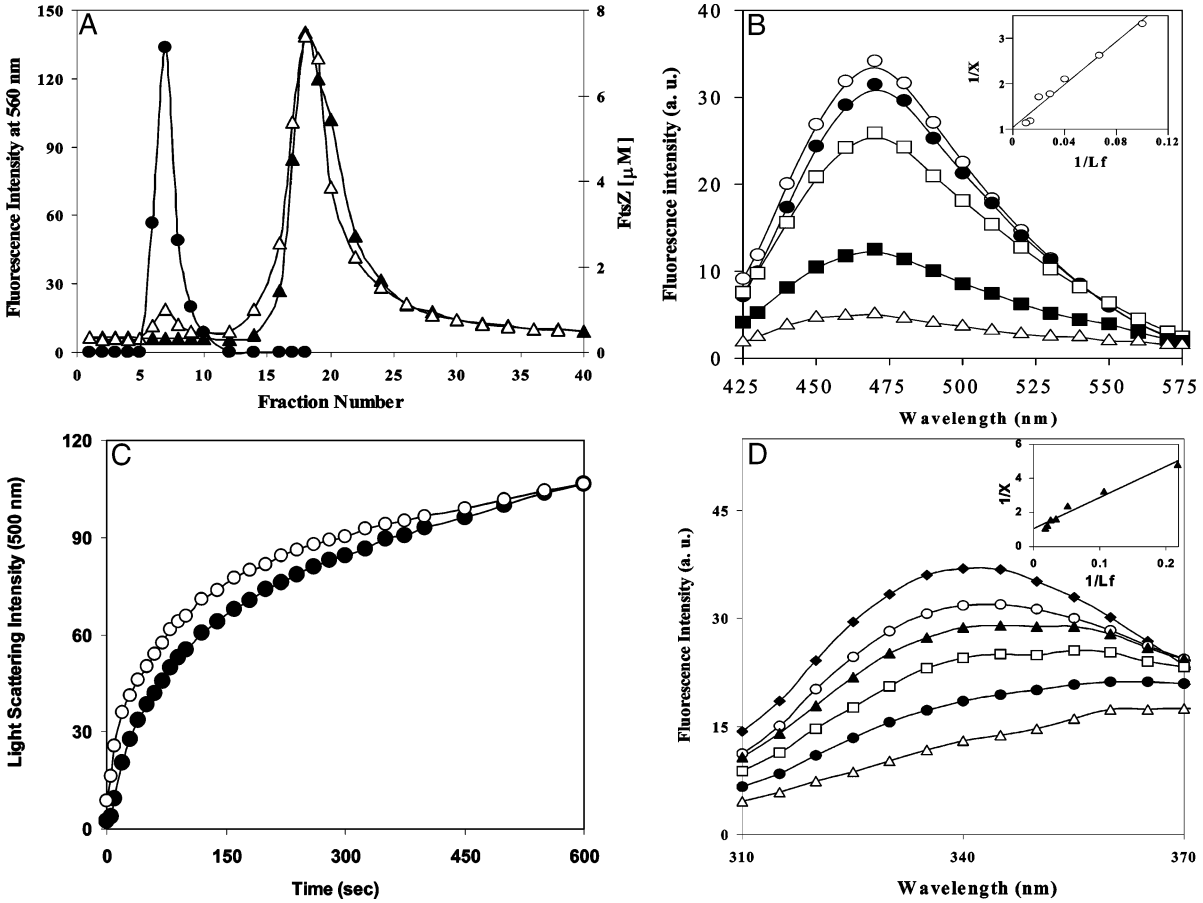

FIGURE 4: Binding of sanguinarine to FtsZ. A shows the elution profile of FtsZ (●), free sanguinarine (▲), and bound sanguinarine (△). FtsZ (20 μM) was incubated with sanguinarine (100 μM) for 30 min at room temperature and passed through a size-exclusion column (as described in the Experimental Procedures). B shows the emission spectra of the FtsZ−ANS complex in the absence (○) and presence of 5 μM (●), 15 μM (□), 50 μM (■), and 75 μM (△) sanguinarine. The inset shows a double-reciprocal plot of the binding data. The excitation and emission wavelength were 370 and 470 nm, respectively. C shows the assembly kinetics of native (○) and mutated FtsZ (●). Native or mutated FtsZ (6 μM) was polymerized in the presence of 10 mM $CaCl_2$, 10 mM $MgSO_4$, and 1 mM GTP at 37 °C. D shows the tryptophan emission spectra in the absence (◆) and presence of 5 μM (○), 10 μM (▲), 20 μM (□), 40 μM (●), and 60 μM (△) sanguinarine. The inset shows a double-reciprocal plot of the binding data. The excitation and emission wavelength were 295 and 340 nm, respectively.

bundling *in vitro*. Therefore, sanguinarine may target FtsZ assembly in the Z ring to inhibit bacterial cytokinesis.

Effects of Sanguinarine on the Cytokinetic Z Ring and Chromosome Organization. The effects of sanguinarine on the cytokinetic Z ring and DNA organization in *B. subtilis* 168 were examined using anti-FtsZ antibodies and DAPI fluorescence (Figure 6). For this experiment, *B. subtilis* 168 was treated with 5 μM sanguinarine for 90 min and immunostained with FtsZ antibody as described in the Experimental Procedures. In the absence of sanguinarine, 12, 64, and 24% of the control cells were found to have one, two, and four nucleoids, respectively. A total of 81% of the *B. subtilis* 168 cells containing two nucleoids were found to have a well-defined Z ring (Table 1). However, control cells containing a single nucleoid did not have a Z ring. The average length of a single nucleoid-containing cell was 1.7 μm, suggesting that these bacteria were newborn. In the presence of 5 μM sanguinarine, 0, 32, 52, and 16% of the cells contained one, two, four, and eight or more nucleoids, respectively. In the presence of 5 μM sanguinarine, no cells were found to contain a single copy of the nucleoid, while 12% of the control population in the absence of sanguinarine contained a single nucleoid, indicating that sanguinarine prevented cytokinesis. Further, we calculated the number of nucleoids/micrometer of the cell length in the absence and presence of different concentrations of sanguinarine (Table 1). The average nucleoids/micrometer of the cell length were found to be similar in the absence and presence of 5 and 8 μM sanguinarine. For example, nucleoids/micrometer cell length were determined to be 0.65 ± 0.11, 0.70 ± 0.18, and 0.64 ± 0.12 in the absence and presence of 5 and 8 μM sanguinarine, respectively (Table 1).

Table 1: Effects of Sanguinarine on the Z Ring and Nucleoids of *B. subtilis* 168[a]

description	control	sanguinarine (5 μM)	sanguinarine (8 μM)
percent of cells with a Z ring	63%	34%	30%
frequency of Z rings/ μm of the cell length	0.22 ± 0.02	0.08 ± 0.01	0.02 ± 0.02
frequency of nucleoids/ μm of the cell length	0.65 ± 0.11	0.70 ± 0.18	0.64 ± 0.12
percent of cells containing two nucleoids	64%	32%	none
percent of cells with two nucleoids having a Z ring	81%	19%	ND
frequency of Z rings/ μm of the cells containing two nucleoids	0.23 ± 0.02	0.05 ± 0.02	ND

[a] A minimum of 200 cells were scored for each concentration of sanguinarine.

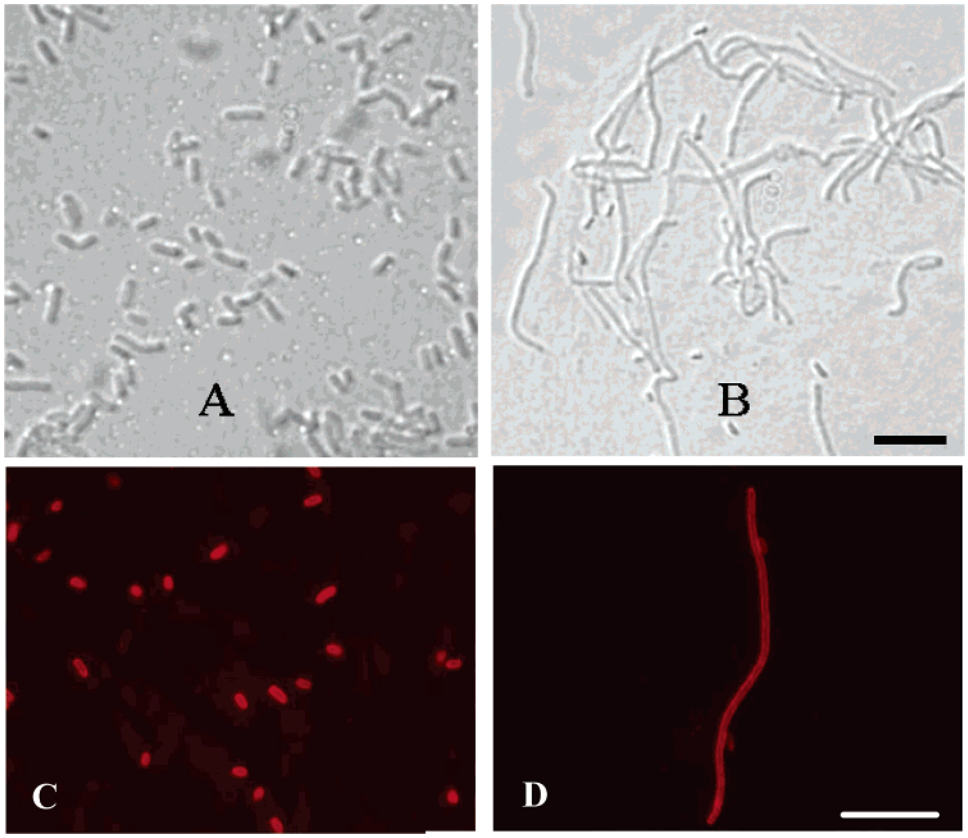

FIGURE 5: Sanguinarine induced filamentation in *B. subtilis* 168. The morphology of *B. subtilis* 168 cells grown overnight in the absence (A) and presence of 5 μM sanguinarine (B) was observed under differential interference contrast microscopy. *E. coli* BL21 cells were grown overnight in the absence (C) and presence of 18 μM sanguinarine (D). Then, the cells were stained with the membrane stain FM 4−64 for 15 min and visualized using a fluorescence microscope. The scale bar is 10 μm in both the cases. The experiment was performed 3 times.

Bacterial populations having two nucleoids were scored by comparing the Z-ring frequencies per *B. subtilis* 168 cell in the absence and presence of sanguinarine. In the presence of 5 μM sanguinarine, only 19% of the cells were found to contain a Z ring. In contrast, 81% of the control cells contained a Z ring. Further, the frequencies of Z ring/micrometer of cell length considering the entire bacterial population were found to be 0.22 ± 0.02, 0.08 ± 0.01, and 0.02 ± 0.02 in the absence and presence of 5 and 8 μM sanguinarine, respectively (Table 1). Sanguinarine not only decreased the frequency of Z-ring occurrence/micrometer of cell length but also perturbed the remaining Z rings (parts C, F, and I of Figure 6). However, no detectable perturbation in DNA condensation and nucleoid segregation was observed in the presence of 5 and 8 μM sanguinarine (parts B, E, and H of Figure 6). The results together suggested that sanguinarine inhibited the formation of the Z ring without affecting the nucleoid segregation.

The effects of sanguinarine on the Z-ring formation were investigated in the *E. coli* WM647 strain that expresses GFP-tagged FtsZ. Cytokinetic Z rings were found to form in all cells in the absence of sanguinarine (Figure 7). Sanguinarine inhibited Z-ring formation in a concentration-dependent manner. For example, the frequency of Z-ring occurrence/micrometer of cell was found to be 0.28 ± 0.02 for the control cells (in the absence of sanguinarine), and the frequencies of Z-ring occurrence were found to be 0.12 ± 0.02 and 0.11 ± 0.01 in the presence of 25 and 50 μM sanguinarine, respectively (Table 2). In other words, the average cell length/Z ring was increased by the sanguinarine. For example, one Z ring was found/3.5 μm of cell length in control cells, whereas one Z ring was found/8.5 μm of cell length in the presence of 25 μM sanguinarine, suggesting that sanguinarine inhibited Z-ring formation. In addition, the Z rings were diffused and perturbed in the presence of sanguinarine.

Table 2: Effects of Sanguinarine on the Z Ring of *E. coli* (JM109 WM647) Were Examined Using GFP-Tagged FtsZ[a]

description	control	sanguinarine (25 μM)	sanguinarine (50 μM)
percent cells having Z ring	90%	55%	45%
frequency of Z ring/μm of length	0.28 ± 0.02	0.12 ± 0.02	0.11 ± 0.01

[a] The frequency of the Z ring was determined by scoring a minimum of 100 cells for each concentration of sanguinarine for each experiment (n = 3).

DISCUSSION

Cell division is considered to be one of the important therapeutic targets for antibacterial drugs (*39*). In this paper, we found that sanguinarine inhibited cytokinesis in both Gram-positive and Gram-negative bacteria by perturbing Z-ring assembly through FtsZ binding. *In vitro*, sanguinarine was found to bind to FtsZ with a dissociation constant of 18−30 μM, and it reduced the light-scattering intensity of FtsZ assembly, decreased sedimentable polymeric mass, and perturbed bundling of FtsZ protofilaments.

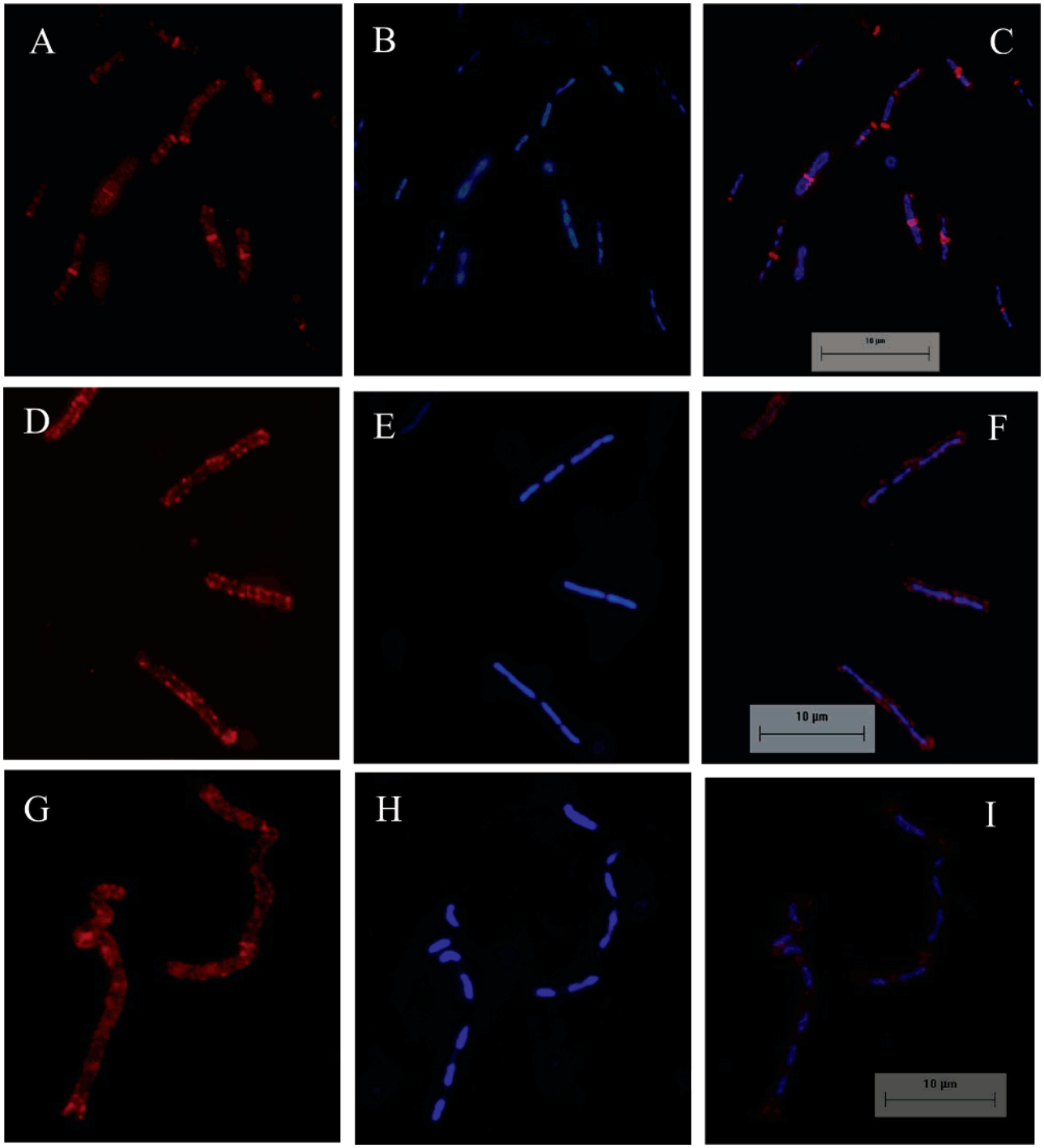

FIGURE 6: Sanguinarine inhibited Z-ring formation but did not affect nucleoid segregation. Cells were immunostained with polyclonal anti-FtsZ rabbit antibody followed by Cy3-conjugated goat anti-rabbit secondary antibody and visualized under fluorescence microscope as described in the Experimental Procedures. Nucleoids were visualized by treating the cells with 0.5 μg/mL DAPI. Z rings are shown in red, and the DAPI-stained nucleoids are shown in blue. Shown are control cells (A and B) and overlay (C), in the presence of 5 μM sanguinarine (D and E) and overlay (F), and in the presence of 8 μM sanguinarine (G and H) and overlay (I). The scale bar is 10 μm.

Sanguinarine increased the average cell length of both *E. coli and B. subtilis* cells, and it also did not perturb the membrane structure in *E. coli*, showing that the antiproliferative activity of sanguinarine was not due to perturbation of the membrane structure. Typical Z rings were visible in *E. coli and B. subtilis*; however, sanguinarine not only reduced the frequency of Z-ring occurrence/unit cell length in these bacteria but also perturbed the Z-ring morphology (parts C, F, and I of Figure 6 and Figure 7). The bacteria with perturbed Z rings could not complete cytokinesis, indicating that the mere presence of a Z ring is not enough for bacterial cell division and that the proper assembly of FtsZ protofilaments may have a role in the functioning of the Z ring.

Although, the average length of *B. subtilis* 168 cells was increased by 5-fold in the presence of sanguinarine, DNA condensation and nucleoid segregation were not perturbed detectably by the compound (Table 1). Further, a population of the sanguinarine-treated *B. subtilis* 168 cells contained 8 nucleoids, whereas no control cells had 8 nucleoids. There-

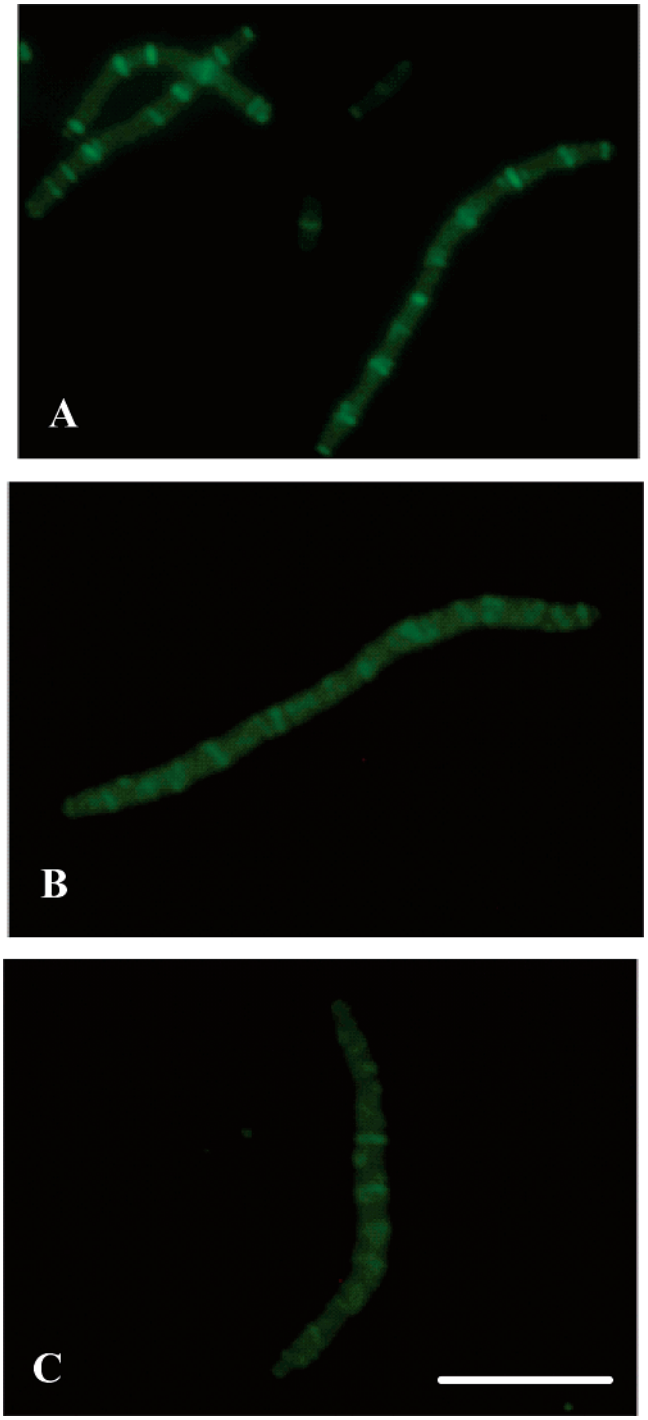

FIGURE 7: Sanguinarine perturbed cytokinetic Z ring in *E. coli*. *E. coli* (JM109 WM647) cells were grown in the LB media containing different concentrations (25−50 μM) of sanguinarine in the presence of 40 μM IPTG. Shown are control cells (A), cells treated with 25 μM (B), and cells treated with 50 μM sanguinarine (C), respectively. Sanguinarine has no auto-fluorescence. The scale bar is 10 μm.

fore, although DNA replication and nucleoid segregation were completed in the presence of sanguinarine, cells were unable to divide because of the perturbation of the cytokinetic Z ring, which produced greater numbers of nucleoids/cell. Using SOS chromotest, sanguinarine has been found to have no genotoxicity in *E. coli* (*40*), which is in agreement with the finding of this paper that sanguinarine does not perturb DNA replication and nucleiod segregation. These data along with the findings of this study support the suggestion that sanguinarine is not acting through an SOS response mechanism.

Sanguinarine inhibited bundling of FtsZ protofilaments. Binding of sanguinarine to FtsZ may induce a conformational change in the protein that weakens the lateral interactions among the protofilaments, which reduce the extent of bundling of protofilaments. Alternatively, the presence of sanguinarine, a bulky polycyclic molecule, on the FtsZ surface may perturb the interaction between the protofilaments by steric hindrance.

The reduction of FtsZ−ANS fluorescence by sanguinarine may be due to either the inhibition of ANS binding to FtsZ, FRET, or the sanguinarine-induced conformational change in the protein (Figure 4B). The dissociation constant of the ANS and FtsZ interaction was found to be 37.4 ± 6.0, 37.1 ± 4.5, and 34.7 ± 7.3 μM in the absence and presence of 25 and 60 μM sanguinarine, respectively. The result suggests that sanguinarine does not bind at the ANS site in FtsZ. The emission spectrum of the FtsZ−ANS complex overlaps significantly with the absorption spectra of sanguinarine, suggesting that they constitute a suitable donor and acceptor pair. Thus, the reduction of FtsZ−ANS fluorescence in the presence of sanguinarine is likely to be due to FRET. However, it is difficult to rule out the possibility that sanguinarine reduces the fluorescence of the FtsZ−ANS complex by inducing a conformational change in FtsZ. The K_d of the sanguinarine and FtsZ interaction was determined to be 18 ± 1.6 and 30 ± 6 μM using the intrinsic tryptophan fluorescence of mutated FtsZ (Y371W) and the extrinsic fluorescence intensity of ANS, respectively. Because sanguinarine did not inhibit the binding of ANS to FtsZ, therefore, the difference in the K_d values is likely to be due to different methods used for determining the K_d.

Sanguinarine has been shown to inhibit the binding of colchicine to tubulin (*20*). Although it is not clear how sanguinarine inhibits tubulin assembly, substantial evidence indicates that colchicine induces a conformational change in tubulin that inhibits microtubule assembly and dynamics (*41*, *42*). Recently, the binding site of colchicine in tubulin has been identified by X-ray crystallography (*41*). Colchicine does not inhibit FtsZ assembly (*37*). Thus, we examined whether the colchicine-binding site is conserved in FtsZ. Because the crystal structure of *E. coli* FtsZ is not known, we used the crystal structure of *Methanococcus janaschii* FtsZ for searching a possible colchicine-binding site in FtsZ. The FtsZ crystal structure (PDB ID: 1FSZ) was superimposed with the β-tubulin crystal structure (PDB ID: 1Z2B) using Swiss-PdbViewer (version 3.7b2), and the amino acid residues that are located within 5 Å proximity to the colchicine molecule in tubulin and FtsZ were identified. Although a colchicine-binding pocket in the FtsZ crystal structure was detected by superposition, the amino acid residues that are in close proximity to colchicine in FtsZ were found to be different from the amino acid residues in tubulin (Table 3). The results may explain why colchicine does not bind to FtsZ. At present, we do not have information about the sanguinarine-binding site in tubulin. Because sanguinarine binds to tubulin and FtsZ, it is possible that the residues that are involved in sanguinarine binding are conserved in both of the proteins.

The assembly dynamics of tubulin, the eukaryotic homologue of FtsZ, have been successfully used as a target for

Table 3: Amino Acid Residues of Tubulin, *M. janaschii* FtsZ, and *E. coli* Lying in Close Proximity to the Colchicine Molecule[a]

β tubulin	*M. janaschii* FtsZ	*E. coli* FtsZ
Val-238		
Thr-239	Leu-222	Ile-196
Cys-241	Leu-225	Leu-199
Leu-242	Ile-226	Val-208
Leu-248	Val-234	Asp-209
Lys-254	Asp-238	Asp-212
Leu-255	Val-239	V-213
Asn-258	Met-243	Met-217
Met-259	Val-242	Val-216
Thr-314	Gly-284	Gly-259
Val-315	Ala-285	Val-260
Ala-316	Leu-286	Leu-261
Ala-317	Ile-287	Val-262
Val-318	His-288	Asn-263
Asn-349	Ala-315	Ala-290
Asn-350	Thr-316	Thr-291
Val-351	Ile-317	Val-292
Lys-352	Ile-318	Val-293
Thr-353	Trp-319	Ile-294
Ala-354	Gly-320	Gly-295
Ile-378		

[a] *M. janaschii* FtsZ (1FSZ) was superimposed with β tubulin (1Z2B). Amino acid residues in the crystal structures lying within 5 Å of the colchicine molecule are shown. The amino acid residues of *E. coli* were identified from the sequence alignment of *M. janaschii* FtsZ and *E. coli* FtsZ (*43*).

developing drugs against several diseases including cancer and fungal diseases. The fact that FtsZ is a conserved as well as an essential protein in almost all prokaryotes and that the conserved properties of FtsZ may not allow the bacteria to develop resistance against FtsZ-targeting drugs together make FtsZ an attractive target for developing novel antimicrobial agents. Sanguinarine does not inhibit proliferation very potently, but it is active against both Gram-positive and Gram-negative bacteria and is also used in a variety of dental products. Thus, sanguinarine may be used as a lead compound to develop more potent antibiotics working by targeting FtsZ. However, sanguinarine has been shown to depolymerize microtubules both *in vitro* and in cancer cells (*20*, *21*). The effects of sanguinarine on microtubules indicate that sanguinarine may have harmful side effects in mammals, which could be a potential drawback in the development of sanguinarine as an antibacterial drug. Further, the results indicate that the bundling of FtsZ protofilaments may play a role in the formation and functioning of the cytokinetic Z ring.

ACKNOWLEDGMENT

T. K. B. and M. K. S. are supported by fellowships from the Council of Scientific and Industrial Research. We thank Dr. William Margolin for providing JM109 (WM647) strain and SAIF, IIT Bombay, for the electron microscopy facility. We thank Dr. Leslie Wilson, Dr. Kenneth H. Downing, and Dr. Patrick A. Curmi for critical reading of the manuscript.

REFERENCES

1. Bi, E. F., and Lutkenhaus, J. (1991) FtsZ ring structure associated with division in *Escherichia coli*, *Nature 354*, 161−164.
2. Rothfield, L., Justice, S., and Garcia-Lara, J. (1999) Bacterial cell division, *Annu. Rev. Genet. 33*, 423−448.
3. Stricker, J., Maddox, P., Salmon, E. D., and Erickson, H. P. (2002) Rapid assembly dynamics of the *Escherichia coli* FtsZ-ring demonstrated by fluorescence recovery after photobleaching, *Proc. Natl. Acad. Sci. U.S.A.* 99, 3171−3175.
4. Addinall, S. G., Bi, E., and Lutkenhaus, J. (1996) FtsZ ring formation in fts mutants, *J. Bacteriol. 178*, 3877−3884.
5. Pinho, M. G., and Errington, J. (2003) Dispersed mode of *Staphylococcus aureus* cell wall synthesis in the absence of the division machinery, *Mol. Microbiol. 50*, 871−881.
6. Lutkenhaus, J., and Addinall, S. G. (1997) Bacterial cell division and the Z ring, *Annu. Rev. Biochem. 66*, 93−116.
7. Lowe, J., van den Ent, F., and Amos, L. A. (2004) Molecules of the bacterial cytoskeleton, *Annu. Rev. Biophys. Biomol. Struct. 33*, 177−198.
8. Addinall, S. G., Cao, C., and Lutkenhaus, J. (1997) Temperature shift experiments with an ftsZ84 (Ts) strain reveal rapid dynamics of FtsZ localization and indicate that the Z ring is required throughout septation and cannot reoccupy division sites once constriction has initiated, *J. Bacteriol. 179*, 4277−4284.
9. Anderson, D. E., Gueiros-Filho, F. J., and Erickson, H. P. (2004) Assembly dynamics of FtsZ rings in *Bacillus subtilis* and *Escherichia coli* and effects of FtsZ-regulating proteins, *J. Bacteriol. 186*, 5775−5781.
10. Wang, J., Galgoci, A., Kodali, S., Herath, K. B., Jayasuriya, H., Dorso, K., et al. (2003) Discovery of a small molecule that inhibits cell division by blocking FtsZ, a novel therapeutic target of antibiotics, *J. Biol. Chem. 278*, 44424−44428.
11. White, E. L., Suling, W. J., Ross, L. J., Seitz, L. E., and Reynolds, R. C. (2002) 2-Alkoxycarbonylaminopyridines: Inhibitors of *Mycobacterium tuberculosis* FtsZ, *J. Antimicrob. Chemother. 50*, 111−114.
12. Reynolds, R. C., Srivastava, S., Ross, L. J., Suling, W. J., and White, E. L. (2004) A new 2-carbamoyl pteridine that inhibits mycobacterial FtsZ, *Bioorg. Med. Chem. Lett. 14*, 3161−3164.
13. Margalit, D. N., Romberg, L., Mets, R. B., Hebert, A. M., Mitchison, T. J., Kirschner, M. W., and RayChaudhuri, D. (2004) Targeting cell division: Small-molecule inhibitors of FtsZ GTPase perturb cytokinetic ring assembly and induce bacterial lethality, *Proc. Natl. Acad. Sci. U.S.A. 101*, 11821−11826.
14. Lu, C., Stricker, J., Erickson, H. P. (2001) Site-specific mutations of FtsZ−Effects on GTPase and *in vitro* assembly, *BMC Microbiol. 1*, 1−7.
15. Erickson, H. P., Taylor, D. W., Taylor, K. A., and Bramhill, D. (1996) Bacterial cell division protein FtsZ assembles into protofilament sheets and minirings, structural homologs of tubulin polymers, *Proc. Natl. Acad. Sci. U.S.A. 93*, 519−523.
16. Koppelman, C. M., Aarsman, M. E., Postmus, J., Pas, E., Muijsers, A. O., Scheffers, D. J., Nanninga, N., and den Blaauwen, T. (2004) R174 of *Escherichia coli* FtsZ is involved in membrane interaction and protofilament bundling, and is essential for cell division, *Mol. Microbiol. 51*, 645−657.
17. Godowski, K. C. (1989) Antimicrobial action of sanguinarine, *J. Clin. Dent. 1*, 96−101.
18. Adhami, V. M., Aziz, M. H., Reagan-Shaw S. R., Nihal, M., Mukhtar, H., and Ahmad, N. (2004) Sanguinarine causes cell cycle blockade and apoptosis of human prostate carcinoma cells via modulation of cyclin kinase inhibitor-cyclin-cyclin-dependent kinase machinery, *Mol. Cancer. Ther.* 3, 933−940.
19. Ahmad, N., Gupta, S., Husain, M. M., Heiskanen, K. M., and Mukhtar, H. (2000) Differential antiproliferative and apoptotic response of sanguinarine for cancer cells versus normal cells. *Clin. Cancer Res. 6*, 1524−1528.
20. Wolff, J., and Knipling, L. (1993) Antimicrotubule properties of benzophenanthridine alkaloids, *Biochemistry 32*, 13334−13339.
21. Slaninova, I., Taborska, E., Bochorakova, H., and Slanina, J. (2001) Interaction of benzo[*c*]phenanthridine and protoberberine alkaloids with animal and yeast cells, *Cell. Biol. Toxicol. 17*, 51−63.
22. de Boer, P., Crossley, R., and Rothfield, L. (1992) The essential bacterial cell-division protein FtsZ is a GTPase, *Nature 359*, 254−256.
23. RayChaudhuri, D., and Park, J. T. (1992) *Escherichia coli* cell-division gene ftsZ encodes a novel GTP-binding protein, *Nature 359*, 251−254.
24. Erickson, H. P. (1995) FtsZ, a prokaryotic homolog of tubulin? *Cell 80*, 367−370.
25. Lowe, J., and Amos, L. A. (1998) Crystal structure of the bacterial cell-division protein FtsZ, *Nature 391*, 203−206.
26. Nogales, E., Downing, K. H., Amos, L. A., and Lowe, J. (1998) Tubulin and FtsZ form a distinct family of GTPases, *Nat. Struct. Biol. 5*, 451−458.

27. Nogales, E., Wolf, S. G., and Downing, K. H. (1998) Structure of the $\alpha\beta$ tubulin dimer by electron crystallography, *Nature 391*, 199−203.
28. Beuria, T. K., Krishnakumar, S. S., Sahar, S., Singh, N., Gupta, K., Meshram, M., and Panda, D. (2003) Glutamate-induced assembly of bacterial cell division protein FtsZ, *J. Biol. Chem. 278*, 3735−3741.
29. Santra, M. K., Beuria, T. K., Banerjee, A., and Panda, D. (2004) Ruthenium red-induced bundling of bacterial cell division protein, FtsZ, *J. Biol. Chem. 279*, 25959−259565.
30. Santra, M. K., and Panda, D. (2003) Detection of an intermediate during unfolding of bacterial cell division protein FtsZ: Loss of functional properties precedes the global unfolding of FtsZ, *J. Biol. Chem*. *278*, 21336−21343.
31. Bradford, M. M. (1976) A rapid and sensitive method for the quantitation of microgram quantities of protein utilizing the principle of protein−dye binding, *Anal. Biochem. 72*, 248−254.
32. Scheffers, D. J., de Wit, J. G., den Blaauwen, T., and Driessen, A. J. (2002) GTP hydrolysis of cell division protein FtsZ: Evidence that the active site is formed by the association of monomers, *Biochemistry 41*, 521−529.
33. Gupta, K., Bishop, J., Peck, A., Brown, J., Wilson, L., and Panda, D. (2004) Antimitotic antifungal compound benomyl inhibits brain microtubule polymerization and dynamics and cancer cell proliferation at mitosis, by binding to a novel site in tubulin, *Biochemistry 43*, 6645−6655.
34. Gupta, K., and Panda, D. (2002) Perturbation of microtubule polymerization by quercetin through tubulin binding: A novel mechanism of its antiproliferative activity, *Biochemistry 41*, 13029−13038.
35. Ma, X., Ehrhardt, D. W., and Margolin, W. (1996) Colocalization of cell division proteins FtsZ and FtsA to cytoskeletal structures in living *Escherichia coli* cells by using green fluorescent protein, *Proc. Natl. Acad. Sci. U.S.A. 93*, 12998-3003.
36. den Blaauwen, T., Buddelmeijer, N., Aarsman, M. E., Hameete, C. M., and Nanninga, N. (1999) Timing of FtsZ assembly in *Escherichia coli*, *J. Bacteriol. 181*, 5167−5175.
37. Yu, X. C., and Margolin, W. (1998) Inhibition of assembly of bacterial cell division protein FtsZ by the hydrophobic dye 5,5-bis-(8-anilino-1-naphthalenesulfonate), *J. Biol. Chem. 273*, 10216−10222.
38. Dai, K., and Lutkenhaus, J. (1991) ftsZ is an essential cell division gene in *Escherichia coli*, *J. Bacteriol*. *173*, 3500−3506.
39. Projan, S. J. (2002) New (and not so new) Antibacterial targets—From where and when will the novel drugs come? *Curr. Opin. Pharmacol. 2*, 513−522.
40. Kevekordes, S., Mersch-Sundermann, V., Burghaus, C. M., Spielberger, J., Schmeiser, H. H., Arlt, V. M., and Dunkelberg, H. (1999) SOS induction of selected naturally occurring substances in *Escherichia coli* (SOS chromotest), *Mutat. Res. 445*, 81−91.
41. Ravelli, R. B., Gigant, B., Curmi, P. A., Jourdain, I., Lachkar, S., Sobel, A., and Knossow, M. (2004) Insight into tubulin regulation from a complex with colchicine and a stathmin-like domain, *Nature 428*, 198−202.
42. Panda, D., Daijo, J. E., Jordan, M. A., and Wilson, L. (1995) Kinetic stabilization of microtubule dynamics at steady state *in vitro* by substoichiometric concentrations of tubulin−colchicine complex, *Biochemistry 34*, 9921−9929.
43. Erickson, H. P. (1998) Atomic structures of tubulin and FtsZ, *Trends Cell Biol. 8*, 133−137.

BI050767+